

Machine learning based optimal control of modular converter for PV assisted power supply systems

Srungaram Ravi Teja¹, Kishore Yadlapati²

¹Department of Electrical and Electronics Engineering, JNTU Kakinada, Kakinada, India

²Department of Electrical and Electronics Engineering, University College of Engineering, Narasaraopet, JNTU Kakinada, Kakinada, India

Article Info

Article history:

Received Dec 14, 2023

Revised Apr 10, 2024

Accepted Jun 20, 2024

Keywords:

Grid integration

Load demand control

MPP tracking

Multilevel inverter

Pattern recognition

PV energy estimation

ABSTRACT

This paper presents the topology and machine learning-based intelligent control of a single-stage grid-connected high-power photovoltaic (PV) system for quality power export to the grid and optimal net energy utilization. A nineteen-level bi-modular inverter is proposed for efficient single-stage PV power conversion. The proposed integrated intelligent machine learning-based control serves for power conversion control as well as supervisory control for hourly PV energy estimation and load demand control for optimal energy consumption. The objectives of power control are extracting maximum power from PV sources and exporting power to the grid at unity power factor. While the objectives for supervisory control are local load demand control for exporting power at higher export prices. The proposed system is implemented using MATLAB/Simulink to validate the efficiency of power conversion, effectiveness of machine learning for energy estimation, and load relay control for optimal energy pricing. The results proved efficient tracking of maximum power, unity power factor at grid terminals, and load relay control for PV energy availability and export cost function.

This is an open access article under the [CC BY-SA](https://creativecommons.org/licenses/by-sa/4.0/) license.



Corresponding Author:

Srungaram Ravi Teja

Department of Electrical and Electronics Engineering, JNTU Kakinada

Kakinada, Andhra Pradesh, India

Email: srungaramraviteja@gmail.com

1. INTRODUCTION

Large scale photovoltaic (PV) integration to grid and PV assisted electric drives demands for optimal energy consumption for efficient usage of renewable PV source. The state-of-art converters for PV integration and PV assisted drives is provided in this section. Also, machine learning algorithms for PV energy estimation and load parameter estimation is reviewed. Single stage conversion of PV power has been developed for efficient conversion and reduction in semi-conductor footprint in power electronic interface [1]. Modular converters are the better choice in this single stage conversion owing to reliability and independent control [2]. Multiple point integration also reduces infrastructure requirements and losses in grid integration [3]. Various unconventional topologies were implemented to minimize the switches or capacitors or diode in the converter. Various non-conventional reduced component count topologies were presented in [4] for drives and renewable energy integration. The un-conventional multilevel generation resorts for utilizing switching circuit connection to synthesize voltage levels in symmetric [5]-[7] with equal voltage levels or asymmetric with unequal voltage levels [8], [9]. In all these converters, the performance is compared in terms of switching power loss, reverse voltage withstand capacity, number and sizing of switches, and power sharing among the modules. Further, adoption of machine learning for renewable system supervisory control [10], [11] and also power flow control is reported for stand alone renewable systems and grid connected renewable systems.

The issues pertaining to synchronization control and fault ride through control under various open and short circuit faults were reported [12], [13], where in possible real-time synchronization issues during grid integration of renewable systems were reported. Mitigation of disturbances pertaining to the quality of power export were dealt in [14], [15]. The machine learning algorithms for PV energy estimation were provided in [16]. Power scheduling based on optimal demand was presented in [17], [18]. Various machine learning applications are developed which include policy approximations for energy management in PV systems [19], energy loss assessment for PV sizing [20], ensemble learning for fault detection in PV systems [21], machine learning for PV energy forecasting [22], clustering and deep learning algorithms for energy estimation [23], Adaline neural networks [24], energy management systems [25], [26], improved forecasting methods for capacity firming [27]. All these technologies and methodologies involve multiple stage conversion, complex algorithms, and convergence.

Therefore, this paper presents machine learning based supervisory and power flow control for PV assisted electrical systems. Current control aspects for a non-conventional, yet modular topology for PV power integration to grid by combining the advantages of reliability, component reduction and single stage power conversion. This paper also presents machine learning based supervisory control for PV energy estimation and corresponding load demand control. The rest of the paper is organized as: i) Section 2 presents the nineteen-level inverter-based topology and control for high power PV systems; ii) Objectives and schemes of integrated intelligent control are presented in section 3; iii) Section 4 presents simulation results and performance validation of the system; and iv) Section 5 presents the conclusion of the paper.

2. SYSTEM DESCRIPTION

The topology of single-stage bi-modular inverter based grid connected photovoltaic (PV) system is depicted in Figure 1. The available PV source is bundled into three strings per each phase which generate voltage levels of 240 V, 80 V, and 40 V which form VPV1, VPV2, and VPV3 respectively. A three phase configuration thus constitutes from nine strings of PV arrays. Bi-modular inverter as shown in Figure 1 which are fed from PV source generate AC voltage with a minimum of seven levels and maximum of nineteen levels in the output voltage. The three-phase voltage thus generated is integrated to grid through LCL filter and transformer. The local loads consist of critical loads for which no interruption in the supply is allowed and time shift allowed category of loads for which load demand control is applied. The structure of bi-modular nineteen-level inverter for single-stage PV conversion is shown in Figure 2 in which module M1 provide lower three levels of output voltage and in combination with module M2 provides the upper 6 levels in each half cycle. The pulse width modulation signals to each switch are generated as follows:

The carrier waveform pertaining to k^{th} switching period is given as (1).

$$V_c(t) = \begin{cases} -1 + \frac{4}{9}(t - kT), (k)T < t \leq (k + \frac{1}{6})T \\ \frac{-25}{27} - \frac{2}{9}(t - (k + \frac{1}{6})T), (k + \frac{1}{6})T < t \leq (k + \frac{1}{3})T \\ \frac{-26}{27} + \frac{4}{9}(t - (k + \frac{1}{3})T), (k + \frac{1}{3})T < t \leq (k + \frac{1}{2})T \\ \frac{-8}{9} - \frac{4}{9}(t - (k + \frac{1}{2})T), (k + \frac{1}{2})T < t \leq (k + \frac{2}{3})T \\ \frac{-26}{27} + \frac{2}{9}(t - (k + \frac{2}{3})T), (k + \frac{2}{3})T < t \leq (k + \frac{5}{6})T \\ \frac{-25}{27} - \frac{4}{9}(t - (k + \frac{5}{6})T), (k + \frac{5}{6})T < t \leq (k + 1)T \end{cases} \quad (1)$$

For $k=0, 1, 2, 3, \dots \infty$. Where, T is time-period for one switching cycle with $\omega_s = \frac{2\pi}{T}$ is the angular switching frequency. Then, the level shifted carrier waveforms are given as (2).

$$V_{(x-9)c}(t) = \frac{x}{9} + V_c(t) \quad (2)$$

For $x=0, 1, 2, \dots, 18$ represent the eighteen level shifted carrier waveforms. The reference sinusoidal signal is given as (3).

$$V_r(t) = M \sin(\omega_r t) \quad (3)$$

With $|M| \leq 1$ and ω_r is the reference angular frequency for output voltage waveform.

The switching instants in each switching period for different carrier waveforms with natural sampling are represented with the following implicit relations, as in (4) and (5).

$$A_{(x-9)k}^a = kT + \frac{T}{4} \left(1 + V_r(A_{(x-9)k}^a) \right) \quad (4)$$

$$B_{(x-9)k}^a = kT + \frac{T}{4} \left(3 - V_r(B_{(x-9)k}^a) \right) \quad (5)$$

Where, $A_{(x-9)k}^a$, and $B_{(x-9)k}^a$ are leading and trailing switching instants of x^{th} carrier in k^{th} switching period.

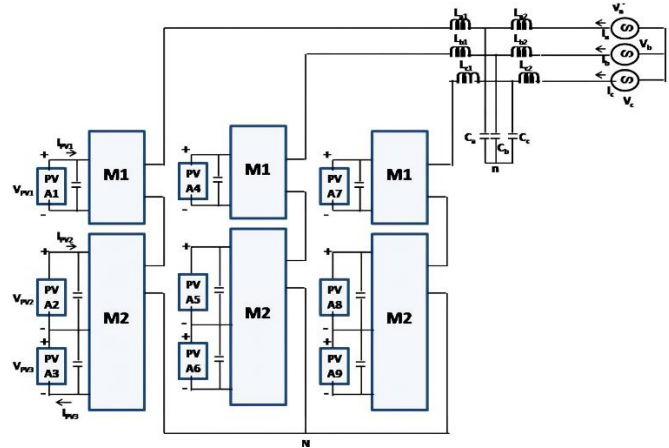


Figure 1. Multi-input point single stage modular PV system

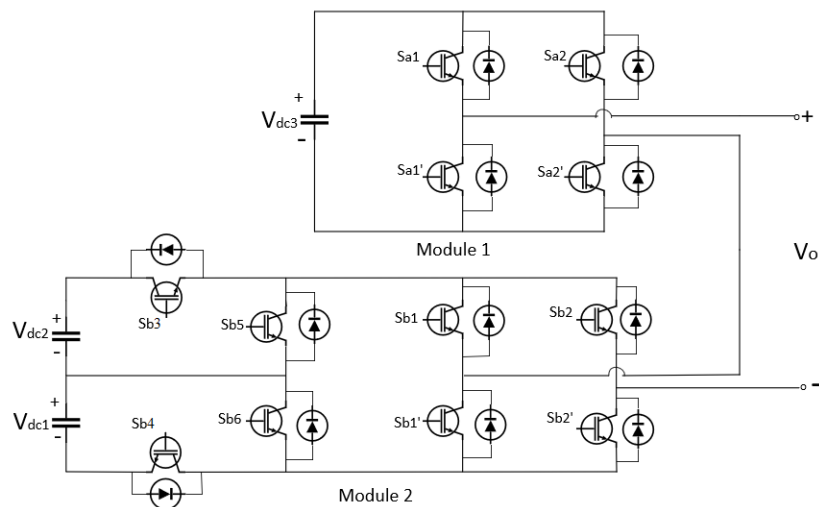


Figure 2. Modular nineteen-level inverter

3. INTEGRATED SUPERVISORY AND POWER FLOW CONTROL

The block diagram of the integrated controller is shown in Figure 3. The power flow control objectives of the integrated controller include extracting maximum power corresponding to irradiance at any given instance and export of power to the grid at unity power factor. The supervisory control objectives include estimation of PV energy for succeeding hour and load demand control through time shifting of allowable loads for optimization of energy pricing for export and import of grid energy.

Voltages and currents of PV arrays are sensed to determine the voltage corresponding to maximum power. Sliding mode control (SMC) is employed for extracting maximum power point (MPP) as shown in Figure 4. The voltage and current are utilized to determine PV array power. The PV power along with gradient of PV power with respective weight functions determine the direction and step size in each iteration to track the maximum power point.

Control of single stage modular inverter is shown in Figure 5. Voltages and currents of grid phase are sensed for current control of modular inverter. The error in obtained direct current (DC) voltage from MPP control and actual PV array voltage serve as input to proportional integral (PI) controller which determine the modulation ratio of the reference sinusoidal current waveform. Artificial neural network (ANN) of pattern recognition model is utilized as machine learning structure to determine the PI controller coefficients. The error in MPP DC voltage and PV array voltage is fed as input to ANN which is trained to generate PI controller coefficients such that error is minimized to zero upon change in irradiance. Sigmoid activation function is used for neurons. A training set of 84 in size with validation set of 15 percent and test set of 15 percent is used. The phase reference is obtained from zero crossing instants of respective phase voltages. The product of these two determines the reference current waveform for each phase. The error in reference and actual currents serve as reference waveform for generating pulse width modulation (PWM) gating signals with level-shifted carries discussed in section 2.

The supervisory control of PV generation estimation and load demand control are achieved through the ANN based algorithm as shown in Figure 6. The pattern recognition ANN network as shown in Figure 7 is utilized for supervisory control. The generalized model was depicted in Figure 7 in which the time varying inputs as an array with multiple features, hidden layers, and output layers to generate required output were identified. The temperature and irradiance serve as inputs for estimation of PV energy production for succeeding hour. The initial values of which are provided and trained with hourly data sets. The weights are updated for optimal value of estimated energy. The same network is also utilized for load demand control for optimal energy pricing. Selling price of energy and purchasing price of energy for the succeeding hour are taken as inputs for the pattern recognition ANN algorithm. The ANN algorithm then determines the optimal schedule of local loads such that net energy pricing is maximized. However, the critical loads are uninterrupted during this schedule. The loads which allow for time shift are assigned priority levels which serve as training data set. The available energy upon optimal energy pricing is determined and based on the priority levels loads are time advanced or delayed for net profit in energy pricing.

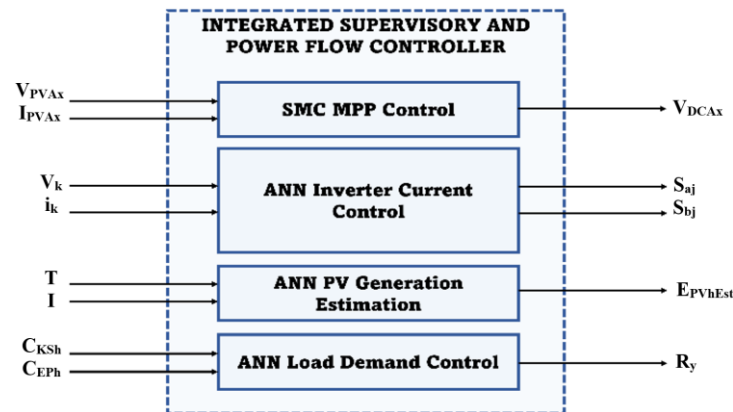


Figure 3. Control block diagram

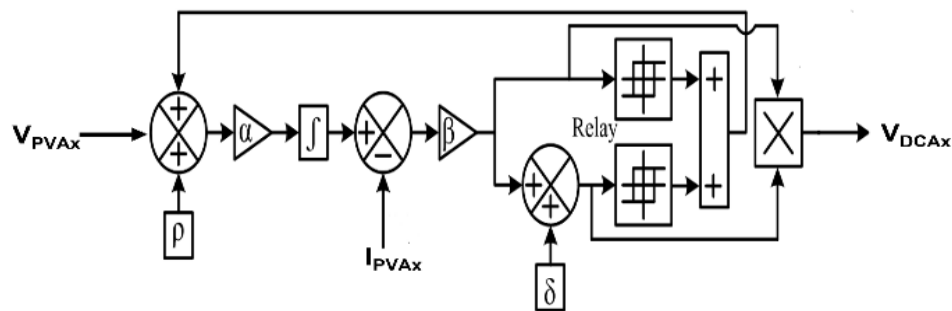


Figure 4. Maximum power point control

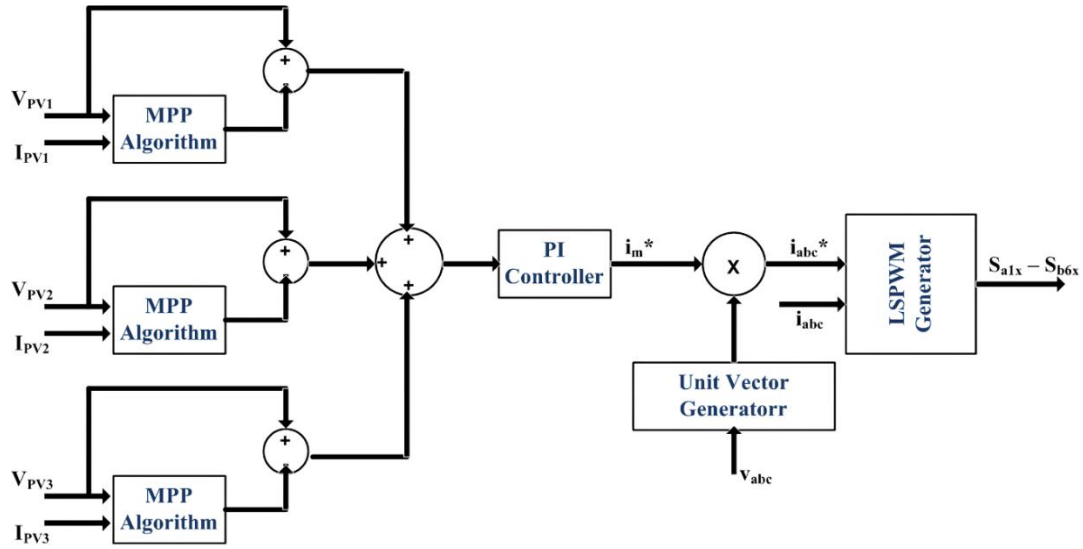


Figure 5. Modular nineteen-level inverter current control

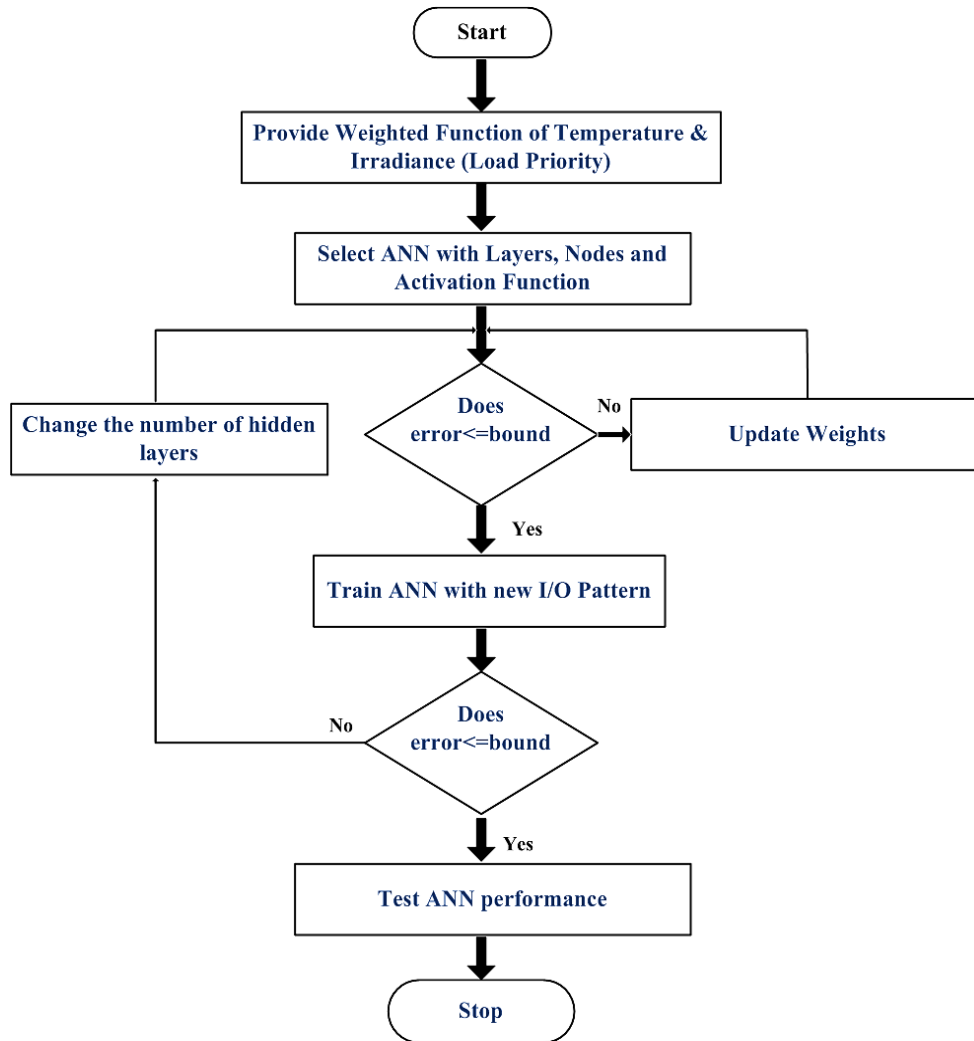


Figure 6. Machine learning algorithm for integrated intelligent control

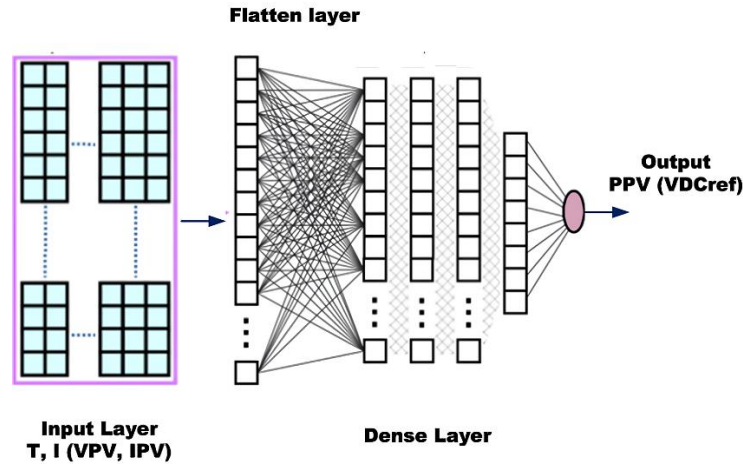


Figure 7. Machine learning scheme for proposed control

4. SIMULATION RESULTS

The proposed topology and integrated control are implemented in MATLAB/Simulink. Simulation parameters are shown in Table 1. The sample priority of loads is shown in Table 2 which depicts the time shift allowed loads and critical loads which serve as parameters to determine optimal energy pricing for estimated hourly PV energy. Hourly data sets of temperature and irradiance with corresponding energy generated by PV arrays on a typical sunny day at Guntur, Andhra Pradesh, India are provided in Table 3. Fifty of such data sets pertaining to different conditions of irradiance and temperature are used for training ANN.

Table 1. Simulation parameters

Parameter	Value
PV power rating	1 MW
V_{PV1} , V_{PV2} , V_{PV3} (for each phase)	40 V, 80 V, 240 V
Rated inverter output voltage	230 V (RMS)
L_1 , L_2	0.18 pu, 0.07 pu
C_3	0.77 pu

Table 2. Load priority

Load type	Priority
Refrigeration	1
Ventilation	1
Illumination	0.7
Air conditioning	0.6
Pumping	0.4

Table 3. Sample training data-hourly data PV for energy estimation

Time interval (HH:MM)	Irradiance (W/m ²)	Temperature (°C)	Normalized power generated (%)
13:00	504	41	25.39472593
13:05	465	41	23.13561481
13:10	465	41	23.13561481
13:15	487	41	24.40998519
13:20	569	42	28.92241481
13:25	505	42	25.21515556
13:30	474	42	23.41945185

4.1. Power flow control

A step change in irradiance from 1000 W/m² to 800 W/m² is created as shown in Figure 8. Following this change in irradiance, V_{PV} and I_{PV} change to new values within 0.4 sec. The power settled to a new maximum value corresponding to 800 W/m² irradiance. Thus, the integrated MPP control is accurate in tracking maximum power for change in irradiance.

The other objective of the power flow control is the modulation of an inverter to export power at the unity factor to the grid. This is realized using single-stage conversion through modulation of inverter instead of regulating D bus. Figure 9 presents the accurate modulation of inverter output voltage for a change in irradiance. Figure 10 presents voltage and current at the grid terminal which depict unity power factor operation. Therefore, it is evident the power is exported to the grid at the unity power factor. Also, the total harmonic distortion is observed to be only 0.7 percent which indicates the efficient conversion.

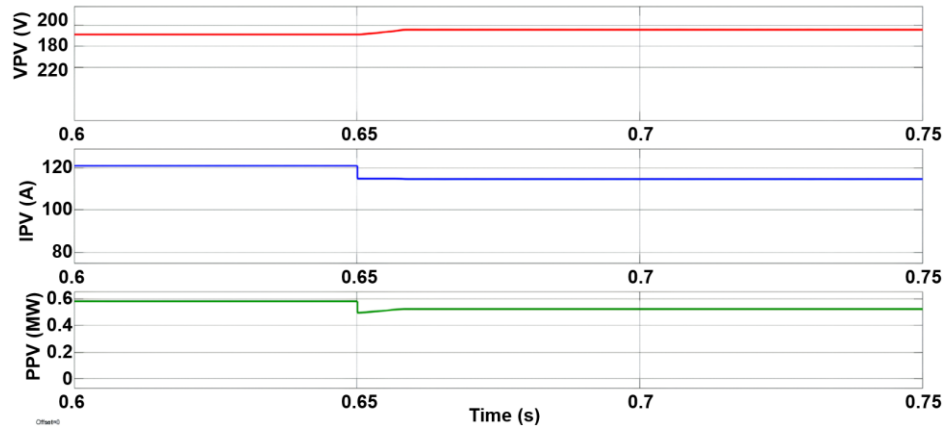


Figure 8. Maximum power point tracking

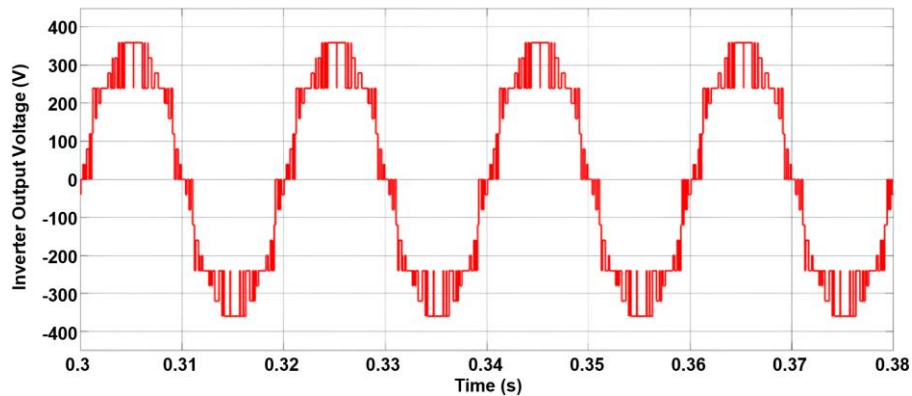


Figure 9. Inverter output voltage

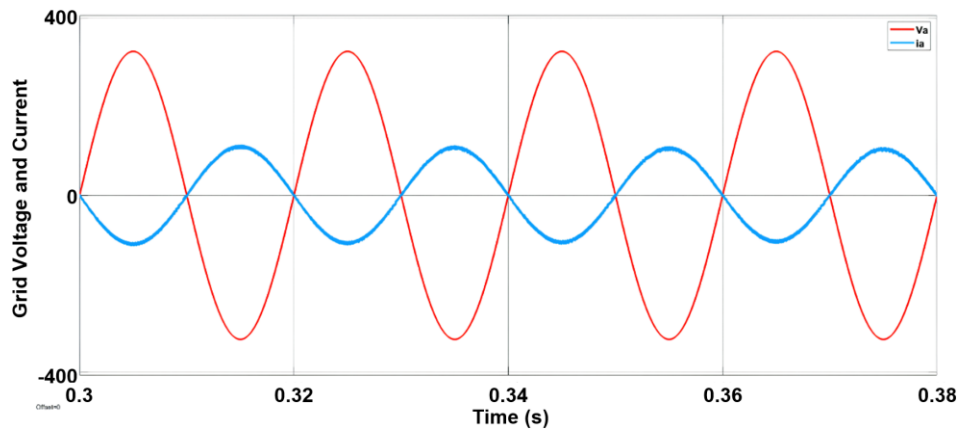


Figure 10. Grid voltage and output current

4.2. Load demand control

The training of ANN for PV energy estimation and load demand control is depicted in Figure 11. The training sets as shown in Table 2 and Table 3 are utilized for machine learning. The convergence was obtained at the eighth iteration of training. The regression for training, validation, and training data sets was observed in Figure 11 which depicts the accuracy to of the training to target output data. The gradient of a mean of squared error and validation checks is shown in Figure 12 which also depicts the convergence of the neural network. The validation of power generation estimation is shown in Figure 13 in which a larger set of instances proved closeness to zero error. The mean squared error shown in Figure 14 indicates a better degree of accuracy in predicting the PV power and load of the proposed ANN control. The load relay pattern for estimated energy and energy pricing for the succeeding hour is shown in Figure 15 which depicts the load to be time-shifted and cut down for the succeeding hour.

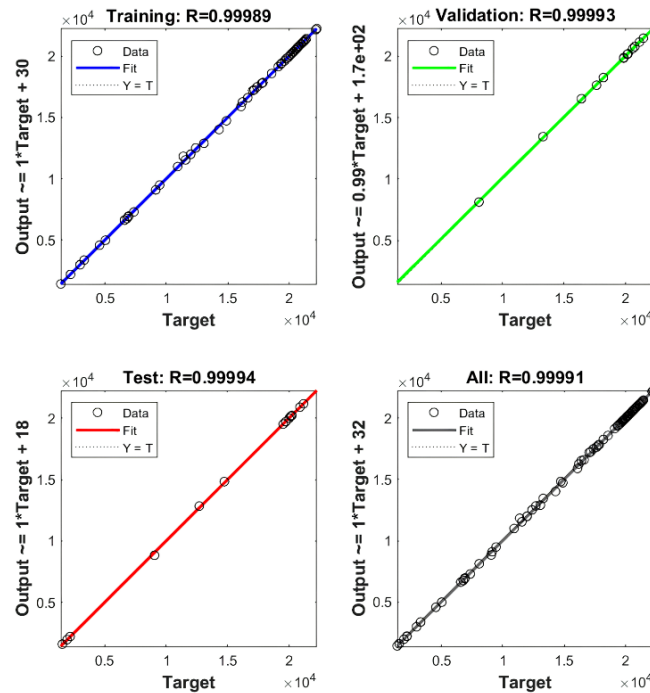


Figure 11. Training ANN for load demand control

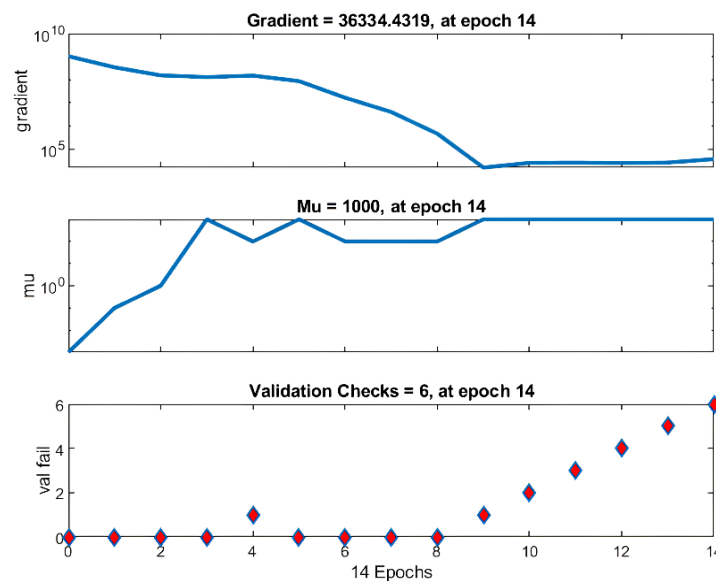


Figure 12. Gradient of mean squared error and validation checks

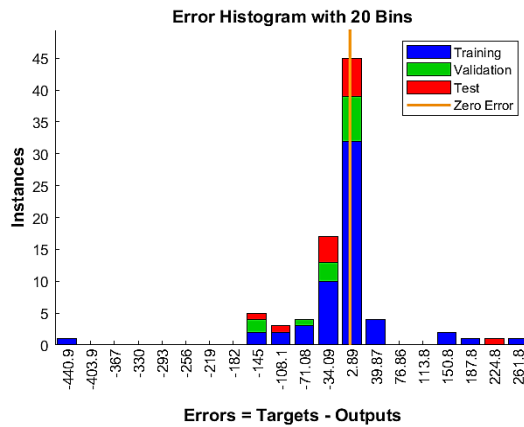


Figure 13. Error histogram for twenty test samples of PV power estimation

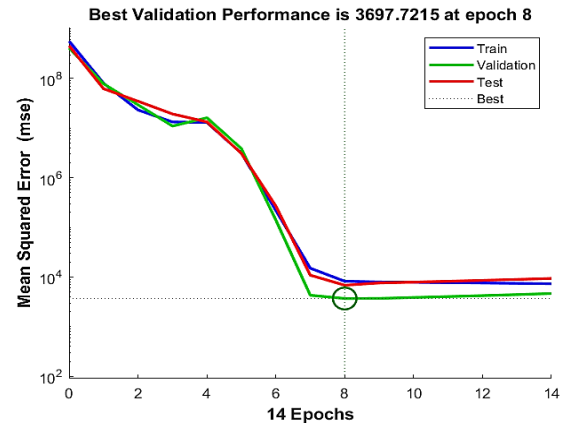


Figure 14. Performance of ANN

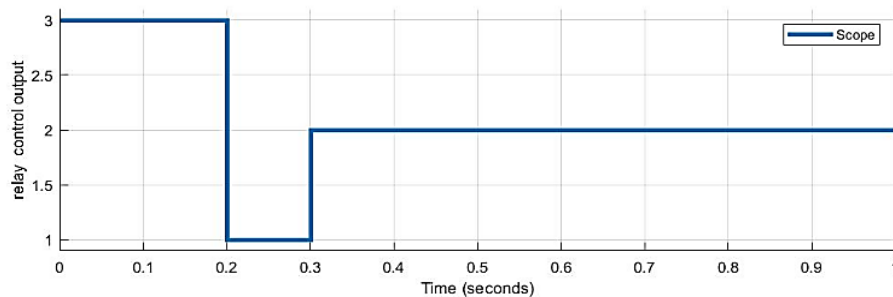


Figure 15. Load relay control

5. CONCLUSION

A multilevel inverter based single stage conversion for high power PV integration to grid is presented in the paper. Also, utilizing the machine learning, a supervisory control strategy to control local loads for optimal power export to grid is developed. The proposed topology and intelligent integrated control proved efficient power conversion with good transient time of 0.25 sec to track new maximum power point and export power to grid at unity power factor with total harmonic distortion of only 0.8 percent. The supervisory control through ANN for PV energy estimation proved accurate estimation with error in actual and predicted value less than 0.01 units. The intelligent controller also determined the load schedule for succeeding hour for optimal energy pricing. Thus, an intelligent control of single stage PV grid integration is achieved with minimal component count and optimal power export.




REFERENCES

- [1] M. J. Sathik, M. F. Elmorshedy, and D. J. Almakhlis, "A new boost topology seven-level inverter of high voltage gain ability and continuous input current with MPPT for PV grid integration," *IEEE Access*, vol. 11, pp. 139236–139248, 2023, doi: 10.1109/ACCESS.2023.3339792.
- [2] F. M. Alhuwaishel, A. K. Allehyani, S. A. S. Al-Obaidi, and P. N. Enjeti, "A medium-voltage DC-collection grid for large-scale PV power plants with interleaved modular multilevel converter," *IEEE Journal of Emerging and Selected Topics in Power Electronics*, vol. 8, no. 4, pp. 3434–3443, Dec. 2020, doi: 10.1109/JESTPE.2019.2934736.
- [3] S. Sivamani, S. P. Mangaiyarkarasi, R. Gandhi Raj, and S. Senthilkumar, "A quad DC source switched three-phase multilevel DC-link inverter topology," *Scientific Reports*, vol. 14, no. 1, p. 2065, Jan. 2024, doi: 10.1038/s41598-024-52605-3.
- [4] A. Srivastava and J. Seshadrinath, "Design and implementation of a new nine level boost inverter for transformerless grid-tied PV application," *IEEE Transactions on Energy Conversion*, vol. 38, no. 4, pp. 2298–2309, Dec. 2023, doi: 10.1109/TEC.2023.3292147.
- [5] P. R. Bana, K. P. Panda, R. T. Naayagi, P. Siano, and G. Panda, "Recently developed reduced switch multilevel inverter for renewable energy integration and drives application: topologies, comprehensive analysis and comparative evaluation," *IEEE Access*, vol. 7, pp. 54888–54909, 2019, doi: 10.1109/ACCESS.2019.2913447.
- [6] H. Samsami, A. Taheri, and R. Samanbakhsh, "New bidirectional multilevel inverter topology with staircase cascading for symmetric and asymmetric structures," *IET Power Electronics*, vol. 10, no. 11, pp. 1315–1323, Sep. 2017, doi: 10.1049/iet-pel.2016.0956.
- [7] S. K. and S. Maiti, "A new multilevel converter configuration with reduced component count for medium voltage STATCOM application," in *2019 National Power Electronics Conference (NPEC)*, IEEE, Dec. 2019, pp. 1–6. doi: 10.1109/NPEC47332.2019.9034699.
- [8] V. S. P. K., S. Peddapati, and S. V. K. Naresh, "A single phase seven-level MLI with reduced number of switches employing a PV Fed SIMO DC-DC converter," in *2020 IEEE Students Conference on Engineering & Systems (SCES)*, IEEE, Jul. 2020, pp. 1–6. doi: 10.1109/SCES50439.2020.9236755.




- [9] A. K. Yadav, K. Gopakumar, K. R. R. L. Umanand, S. Bhattacharya, and W. Jarzyna, "A hybrid 7-level inverter using low-voltage devices and operation with single DC-Link," *IEEE Transactions on Power Electronics*, vol. 34, no. 10, pp. 9844–9853, Oct. 2019, doi: 10.1109/TPEL.2018.2890371.
- [10] C. Dhananjayulu, P. Kaliannan, S. Padmanaban, P. K. Maroti, and J. B. Holm-Nielsen, "A new three-phase multilevel asymmetrical inverter with optimum hardware components," *IEEE Access*, vol. 8, pp. 212515–212528, 2020, doi: 10.1109/ACCESS.2020.3039831.
- [11] S. J. Gambhire, M. K. Kumar, K. Mallikarjuna, A. N. Venkateswarlu, Ch. N. S. Kalyan, and B. S. Goud, "Performance comparison of various classical controllers in LFC of hydro-thermal power system with time delays," in *2022 10th International Conference on Smart Grid (icSmartGrid)*, IEEE, Jun. 2022, pp. 401–406. doi: 10.1109/icSmartGrid55722.2022.9848690.
- [12] C. R. Reddy, B. S. Goud, F. Aymen, G. S. Rao, and E. C. Bortoni, "Power quality improvement in hres grid connected system with FOPID based atom search optimization technique," *Energies (Basel)*, vol. 14, no. 18, p. 5812, Sep. 2021, doi: 10.3390/en14185812.
- [13] H. Gaied *et al.*, "Comparative analysis of MPPT techniques for enhancing a wind energy conversion system," *Frontiers in Energy Research*, vol. 10, Aug. 2022, doi: 10.3389/fenrg.2022.975134.
- [14] Ch. R. Reddy, B. S. Goud, B. N. Reddy, M. Pratyusha, C. V. V. Kumar, and R. Rekha, "Review of islanding detection parameters in smart grids," in *2020 8th International Conference on Smart Grid (icSmartGrid)*, IEEE, Jun. 2020, pp. 78–89. doi: 10.1109/icSmartGrid49881.2020.9144923.
- [15] R. Barzegarkhoo, S. A. Khan, Y. P. Siwakoti, R. P. Aguilera, S. S. Lee, and Md. N. H. Khan, "Implementation and analysis of a novel switched-boost common-ground five-level inverter modulated with model predictive control strategy," *IEEE Journal of Emerging and Selected Topics in Power Electronics*, vol. 10, no. 1, pp. 731–744, Feb. 2022, doi: 10.1109/JESTPE.2021.3068406.
- [16] G. Grusso and G. S. Gajani, "Comparison of machine learning algorithms for performance evaluation of photovoltaic energy forecasting and management in the TinyML framework," *IEEE Access*, vol. 10, pp. 121010–121020, 2022, doi: 10.1109/ACCESS.2022.3222986.
- [17] D. Iannuzzi, M. Coppola, P. Guerriero, A. Dannier, and A. Del Pizzo, "Power scheduling method for grid integration of a PV-BESS CHB inverter with SOC balancing capability," *IEEE Access*, vol. 10, pp. 112273–112285, 2022, doi: 10.1109/ACCESS.2022.3215270.
- [18] S. R. Pendem, S. Mikkili, and P. K. Bonthagorla, "PV distributed-MPP tracking: total-cross-tied configuration of string-integrated-converters to extract the maximum power under various PSCs," *IEEE Systems Journal*, vol. 14, no. 1, pp. 1046–1057, Mar. 2020, doi: 10.1109/JSYST.2019.2919768.
- [19] C. Keerthisinghe, A. C. Chapman, and G. Verbic, "Energy management of PV-storage systems: policy approximations using machine learning," *IEEE Transactions on Industrial Informatics*, vol. 15, no. 1, pp. 257–265, Jan. 2019, doi: 10.1109/TII.2018.2839059.
- [20] K. Mahmoud and M. Abdel-Nasser, "Fast yet accurate energy-loss-assessment approach for analyzing/sizing PV in distribution systems using machine learning," *IEEE Transactions on Sustainable Energy*, vol. 10, no. 3, pp. 1025–1033, Jul. 2019, doi: 10.1109/TSTE.2018.2859036.
- [21] K. Dhibi, M. Mansouri, K. Bouzrara, H. Nounou, and M. Nounou, "An enhanced ensemble learning-based fault detection and diagnosis for grid-connected PV systems," *IEEE Access*, vol. 9, pp. 155622–155633, 2021, doi: 10.1109/ACCESS.2021.3128749.
- [22] K. Mahmud, S. Azam, A. Karim, S. Zobaed, B. Shanmugam, and D. Mathur, "Machine learning based PV power generation forecasting in alic springs," *IEEE Access*, vol. 9, pp. 46117–46128, 2021, doi: 10.1109/ACCESS.2021.3066494.
- [23] S. M. Mirafabzadeh, M. Longo, and M. Brenna, "Knowledge extraction from PV power generation with deep learning autoencoder and clustering-based algorithms," *IEEE Access*, vol. 11, pp. 69227–69240, 2023, doi: 10.1109/ACCESS.2023.3292516.
- [24] A. A. Jai and M. Ouassaid, "Machine learning-based Adaline neural PQ strategy for a photovoltaic integrated shunt active power filter," *IEEE Access*, vol. 11, pp. 56593–56618, 2023, doi: 10.1109/ACCESS.2023.3281488.
- [25] G. Tziolis, A. Livera, J. Montes-Romero, S. Theocharides, G. Makrides, and G. E. Georgiou, "Direct short-term net load forecasting based on machine learning principles for solar-integrated microgrids," *IEEE Access*, vol. 11, pp. 102038–102049, 2023, doi: 10.1109/ACCESS.2023.3315841.
- [26] M. M. Shibl, L. S. Ismail, and A. M. Massoud, "An intelligent two-stage energy dispatch management system for hybrid power plants: impact of machine learning deployment," *IEEE Access*, vol. 11, pp. 13091–13102, 2023, doi: 10.1109/ACCESS.2023.3243097.
- [27] C. Keerthisinghe, E. Mickelson, D. S. Kirschen, N. Shih, and S. Gibson, "Improved PV forecasts for capacity firming," *IEEE Access*, vol. 8, pp. 152173–152182, 2020, doi: 10.1109/ACCESS.2020.3016956.

BIOGRAPHIES OF AUTHORS



Srungaram Ravi Teja    is research scholar at JNTU Kakinada and assistant professor in Electrical and Electronics Engineering Department at KL deemed to be University, Guntur, Andhra Pradesh, India. He received his B.Tech. degree in Electrical and Electronics Engineering from JNTUK in 2012 and M.Tech. degree in Electrical Engineering from NIT Warangal in 2015. His research interests include the field of power electronics, motor drives, renewable energy, FPGA applications, embedded systems, artificial intelligence, intelligent control, and digital library. He can be contacted at email: srungaramraviteja@gmail.com.



Kishore Yadlapati    received B.Tech. (Electrical and Electronics Engineering) from ANU Guntur (1999), M.E. (Power Electronics) from RGPVVV (2001), Bhopal and Ph.D. in Electrical and Electronics Engineering from JNTU Hyderabad (2015). He is currently working as associate professor and head of the Department of EEE at University College of Engineering Narasaraopet JNTUK Kakinada. His research interests are in the areas of control and estimation of induction motor drives, integration of renewable sources of energy to grid, and switch mode power supplies. He is a life member of ISTE and senior member of IEEE. He can be contacted at email: kyadlapati@ieee.org.